# Supporting information

## Pressure-induced pseudorotation in crystalline pyrrolidine

***Kamil F. Dziubek and Andrzej Katrusiak***

*Faculty of Chemistry, Adam Mickiewicz University, Grunwaldzka 6, 60-780 Poznań, Poland*

## Experimental procedures

*Loading a diamond anvil cell and crystal growth*

Pyrrolidine (Aldrich, ≥ 99 % purity) was used without further purification. A single crystal of pyrrolidine was grown in situ in a four-bolt diamond anvil cell (DAC) equipped with beryllium backing seats and 0.8 mm culet diamond anvils. The gasket was made of 0.20 thick steel foil preindented to 0.12 mm, with the spark-eroded hole 0.33 mm in diameter. After filling the chamber, DAC was closed and pressure slowly increased. Since the sample vitrification occurred, in next attempts pressure was increased stepwise and after each cycle the sample was left overnight to allow time for nucleation of crystallites. Eventually, pyrrolidine froze forming a polycrystalline mass. Then the DAC was heated with a hot-air gun until all grains but one melted, after which it was cooled down slowly and the seed formed a single crystal filling entirely the experimental chamber at 1.5 GPa. Pressure was calibrated by measuring the shift of the R1 ruby fluorescence line[1] using a BETSA PRL spectrometer with an accuracy of 0.05 GPa. At higher pressure a single-crystal growth was hampered by strongly increased viscosity of the sample.

*In situ cryocrystallization*

The low-temperature single-crystal X-ray diffraction experiments for pyrrolidine were performed in a glass capillary, 0.3 mm in diameter. Temperature was controlled by an Oxford Diffraction Cryosystems CPC611 low-temperature attachment. The capillary was mounted on a diffractometer and cooled down. Pyrrolidine froze at 210 K. Then temperature was cycled close to the melting point and the sample monitored visually and by recording 30 s X-ray diffraction images. After several attempts a single crystal suitable for diffraction experiments was grown.

*Data collection and reduction*

Diffraction data were collected on a KUMA KM4 diffractometer equipped with a CCD detector and a monochromated Mo sealed-tube source (Kα radiation, λ = 0.71073 Å). The low-temperature (LT) diffraction data were collected at 100 K and 200 K. The alignment of DAC was performed using a gasket-shadow centering procedure.[2] High-pressure (HP) data collection was carried out using a pre-designed strategy combining $\omega$- and $\phi$-scans.[2] The CrysAlisPro program suite[3] was used for data collection, determination of the UB-matrices, initial data reduction, and Lp correction. The reflection intensities from the high pressure experiment were additionally corrected for the DAC absorption and gasket shadowing[4], and the diamond-anvil reflections were eliminated. The structures were solved straightforwardly using direct methods (SHELXS-97) and subsequently refined against $F^2$ with SHELXL-97[5]. The N- and C-atoms were refined with anisotropic (LT) and isotropic (HP) displacement parameters, and the isotropic displacement parameters of the H-atoms were set to 1.2 times the $U_{eq}$ or $U_{iso}$ of their carrier atoms, respectively. In LT structures all hydrogen atom

positions were refined, while in the HP structure C-H hydrogen atoms were located at geometrically idealized positions using the AFIX 23 command of the SHELXL-97 program; the N-H hydrogen atoms were unconstrained during the refinement. The refinement and experimental details are presented in Table S1.

Molecular graphics, Hirshfeld surfaces and structural dimensions

Molecular graphics were prepared using X-Seed software.[6] Hirshfeld fingerprint plots were produced with CrystalExplorer.[7,8] The structural data of phase $\alpha$ at 100 K / 0.1 MPa were used for preparing Figures 1-3 and S1-S2, Tables 1 and S4, and for the PIXEL quantum-chemistry potential energy calculations.

PIXEL calculations

The molecular structures determined by X-ray crystallography (with neutron-normalized H-atom positions[9]) were used to calculate the molecular electron density using the program GAUSSIAN03[10] at the MP2/6-31G** level of theory, which was shown to perform well for calculating molecular electron density used further in the PIXEL approach[11]. These electron density models were subsequently used for PIXEL calculations using OPiX program package[12], which allows the evaluation of pairwise molecule-molecule interactions and lattice energies, broken down into Coulombic, polarization, dispersion and repulsion components. Lattice energy calculations employed a cluster of molecules of radius 14 Å. Noteworthy, the polarization energy is not additive over pairs; hence the energies for singled-out pairs do not sum up to the total polarization (due to many-body effects)[13]. However, conclusions on the relative strength of bonding contributions in crystals are valid because the differences with true energies are relatively small, in particular concerning the strongest interactions.
According to the results of PIXEL calculations (Table S2), the interaction energy between N6H6···N1 bonded molecules remains unchanged compared to phase $\alpha$ (the N6H6···N1 bond dimensions remain unchanged), while shortening of the N1H1···N6 bond increases its energy by 5.0 kJ/mol. Thus the difference in hydrogen bond energy on transition to phase $\beta$ is 2.5 kJ/mol, where one per two H-bonds changes its energy. The conformational interconversion of molecule B constitutes about 5%, H-bond energy change 40 %, and the largest of remaining 55% is mostly due to the compression of van der Waals contacts (Table S3).

Table S1. Crystal data and details of structure refinement for pyrrolidine.

| phase | $\alpha$ | $\alpha$ | $\beta$ |
|---|---|---|---|
| temperature(K) | 100(2) | 200(2) | 295(2) |
| pressure (GPa) | 0.0001 | 0.0001 | 1.50(5) |
| crystal size (mm) | 0.30x0.30x0.30 | 0.30x0.30x0.30 | 0.12x0.33x0.33 |
| crystal system | monoclinic | monoclinic | triclinic |
| space group | $P2_1/c$ | $P2_1/c$ | $P\bar{1}$ |
| unit cell dimensions (Å) | $a$ = 8.6367(6) | $a$ = 8.717(2) | $a$ = 7.702(2) |
| | $b$ = 5.2081(3) | $b$ = 5.233(1) | $b$ = 4.938(1) |
| | $c$ = 10.6375(8) | $c$ = 10.831(2) | $c$ = 10.572(2) |
| | $\beta$ = 110.579(8) | $\beta$ = 110.45(3) | $\alpha$ = 94.37(3) |
| | | | $\beta$ = 98.54(3) |
| | | | $\gamma$ = 99.59(3) |
| volume (Å$^3$) | 447.95(5) | 462.93(19) | 389.96 (15) |
| $Z$ | 4 | 4 | 4 |
| $\rho_{calcd}$ (g cm$^3$) | 1.055 | 1.193 | 1.211 |
| $\mu$ (Mo K$_\alpha$) (mm$^{-1}$) | 0.06 | 0.07 | 0.07 |
| F(000) (e) | 160 | 160 | 160 |
| 2$\theta$ max (º) | 59.35 | 59.60 | 49.76 |
| 2$\theta$ range (º) | 5.04-59.35 | 4.98-59.60 | 5.44-49.76 |
| limiting indices | -11→h→10 | -11→h→10 | -9→h→9 |
| | -7→k→5 | -7→k→5 | -5→k→5 |
| | -14→l→14 | -13→l→14 | -5→l→6 |
| reflections collected/unique | 4396 / 1184 | 2975 / 1187 | 2002 / 434 |
| $R_{int}$ | 0.0142 | 0.0722 | 0.0848 |
| observed reflections [$I > 4\sigma(I)$] | 987 | 712 | 259 |
| data/parameters | 1184 / 73 | 1187 / 73 | 434 / 47 |
| goodness of fit ($F^2$) | 1.041 | 1.005 | 1.055 |
| final $R$ indices ($I > 4\sigma(I)$) | 0.0361 | 0.0629 | 0.0764 |
| $\Delta\sigma_{max}$, $\Delta\sigma_{min}$ (e Å$^3$) | 0.30 / -0.15 | 0.22 / -0.37 | 0.12 / -0.14 |
| DAC transmission min/max | - | - | 0.630 / 0.871 |
| gasket shadowing min/max | - | - | 0.695 / 0.959 |
| total transmission | - | - | 0.438 / 0.826 |

Table S2. Donohue angles for NH···N hydrogen bonds in pyrrolidine phases *α* (at 100 K/0.1 MPa) and *β* (at 295 K/1.5 GPa), plotted in Figure 2 in the main article. Symmetry codes: (i) 1-x, y-0.5, 0.5-z; (ii) x, y-1, z.

| Phase *α* | |
|---|---|
| C2-N1···N1$^{i}$ (º) | 96.27(12) |
| C5-N1···N1$^{i}$ (º) | 107.2(12) |
| N1···N1$^{i}$-C2$^{i}$ (º) | 130.7(14) |
| N1···N1$^{i}$-C5$^{i}$ (º) | 106.0(13) |
| Phase *β* | |
| C2-N1···N6 (º) | 95.7(8) |
| C5-N1···N6 (º) | 101.0(5) |
| N1···N6-C7 (º) | 117.9(9) |
| N1···N6-C10 (º) | 121.4(9) |
| C7-N6···N1$^{ii}$ (º) | 115.9(6) |
| C10-N6···N1$^{ii}$ (º) | 90.0(7) |
| N6···N1-C2$^{ii}$ (º) | 102.9(6) |
| N6···N1-C5$^{ii}$ (º) | 140.2(10) |

Table S3. Lattice and molecule-molecule interaction energies calculated using PIXEL method for pyrrolidine phases *α* (at 100 K, 0.1 MPa) and *β* (at 295 K, 1.5 GPa). Symmetry codes: (i) 1-x, y-0.5, 0.5-z; (ii) x, y-1, z.

| | coulombic energy (kJ/mol) | polarization energy (kJ/mol) | dispersion energy (kJ/mol) | repulsion energy (kJ/mol) | total energy (kJ/mol) |
|---|---|---|---|---|---|
| Lattice energies | | | | | |
| Phase α | –34.5 | –16.0 | –61.3 | 60.2 | –51.7 |
| Phase β | –47.2 | –24.2 | –86.8 | 112.8 | –45.4 |
| Molecule-molecule interaction energies | | | | | |
| Phase α | | | | | |
| N1-H1···N1$^{i}$ | –24.5 | –9.9 | –14.1 | 30.8 | –17.7 |
| Phase β | | | | | |
| N1-H1···N6 | –29.5 | –13.7 | –18.6 | 49.1 | –12.7 |
| Phase β | | | | | |
| N6-H6··· N1$^{ii}$ | –23.9 | –9.9 | –18.1 | 34.3 | –17.7 |

Table S4. The potential energy ($E_p$) balance for phases $\alpha$ and $\beta$. $\Delta E_p$ is the increase of $E_p$ between phases $\alpha$ (at 100 K, 0.1 MPa) and $\beta$ (at 295 K, 1.5 GPa), with its conformational, hydrogen bond and van der Waals components specified (as indicated in parentheses). The potential energy fractions, $\Delta E_p/\Delta E_p$ (total), have been calculated for the contributing $\Delta E_p$ magnitudes averaged for two symmetry-independent molecules in phase $\beta$: e.g. $\Delta E_p/\Delta E_p$ (total) of 2 % is obtained from conformational energies of 0 and 0.3 divided by 6.3 kJ/mol.

| $\Delta E_p$ | $E_p$ difference (kJ/mol) | $\Delta E_p/\Delta E_p$ (total) |
|---|---|---|
| $\Delta E_p$ (conformation) | molecule A 0<br>molecule B[i] 0.3 | 2% |
| | molecule A 0<br>molecule B[ii] 0.8 | 6% |
| | molecule A 0<br>molecule B[iii] 0.75 | 4% |
| | molecule A 0<br>molecule B[iii] 0.51 | 6% |
| $\Delta E_p$ (hydrogen bond)[iv] | H-bond A···B 5.0<br>H-bond B···A 0 | 40% |
| $\Delta E_p$ (van der Waals)[v] | 3.65[i] | 58% |
| | 3.4[ii] | 54% |
| | 3.545[iii] | 56% |
| | 3.425[iii] | 54% |
| $\Delta E_p$ (total)[iv] | 6.3 | 100% |

[i] Calculated at the B3LYP/aug-cc-pVDZ level.[14]

[ii] Calculated at the MP2/aug-cc-pVDZ level.[14]

[iii] Taken as the femtosecond degenerate four-wave mixing spectroscopy results with an error estimate (0.63±0.12 kJ/mol).[14]

[iv] From PIXEL[12] calculations (cf. Table S2).

[v] Calculated as a difference between the total lattice energy and hydrogen-bond energy changes.

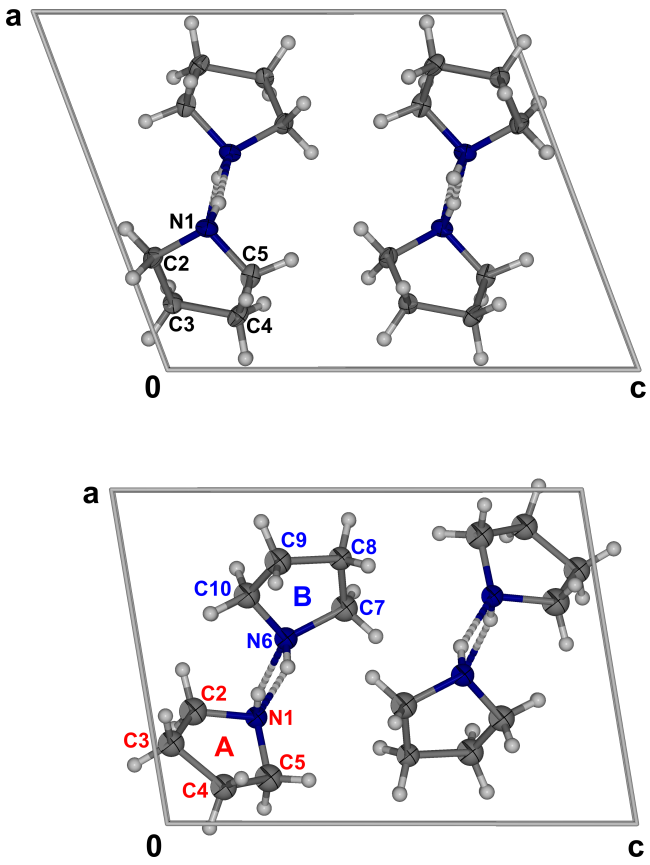


***Figure S1.*** The crystal packing of the NH···N bonded chains in pyrrolidine phases : (a) projected down ***b*** in phase $\alpha$ ; and (b) down ***b*** in phase $\beta$. Capital letters A and B denote symmetry-independent molecules in phase $\beta$.

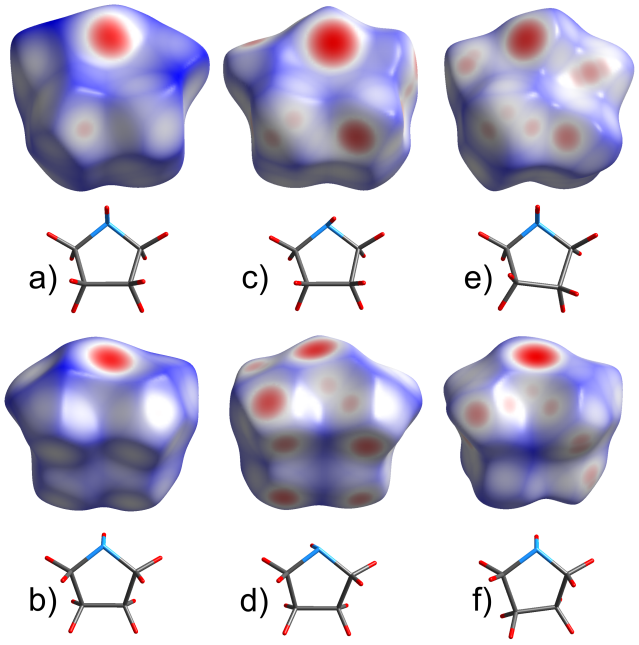


***Figure S2.*** Hirshfeld surfaces decorated with normalized contact distance ($d_{norm}$) based on the sums of van der Waals radii[8], ranging from –0.5 Å (red) to 1.2 Å (blue) for a molecules in phase $\alpha$ (a-b), and molecules A (c-d) and B (e-f) in phase $\beta$.

*References*

(1) Piermarini, G. J.; Block, S.; Barnett, J. D.; Forman, R. A. *J. Appl. Phys.* **1975**, *46*, 2774−2780.
(2) Budzianowski, A.; Katrusiak A. In *High-Pressure Crystallography*; Katrusiak, A., McMillan, P. F., Eds.; Kluwer: Dordrecht, the Netherlands, **2004**; pp 157−168.
(3) Xcalibur CCD System, CrysAlisPro Software System, version 1.171.34; Oxford Diffraction Ltd.: Wrocław, Poland, **2010**.
(4) Katrusiak, A. *REDSHADE, A program for correcting reflections intensities for DAC absorption and gasket shadowing*; Adam Mickiewicz University: Poznań, Poland, **2003**.
(5) Sheldrick, G. M. *Acta Crystallogr., Sect. A* **2008**, *64*, 112–122.
(6) Barbour, L. J. *J Supramol. Chem.* **2001**, *1*, 189–191.
(7) Wolff, S. K.; Grimwood, D. J.; McKinnon, J.J.; Turner, M.J.; Jayatilaka, D.; Spackman, M.A. CrystalExplorer (Version 2.2), University of Western Australia, Perth, **2010**.
(8) McKinnon, J. J.; Jayatilaka, D.; Spackman, M.A. *Chem. Commun.* **2007** ,3814–3816.
(9) Allen, F. H.; Bruno, I. J. *Acta Crystallogr., Sect. B* **2010**, *66*, 380–386.
(10) Frisch, M. J.; Trucks, G. W.; Schlegel, H. B.; Scuseria, G. E.; Robb, M. A.; Cheeseman, J. R.; Montgomery, J. A.; Vreven, T.; Kudin, K. N.; Burant, J. C.; Millam, J. M.; Iyengar, S. S.; Tomasi, J.; Barone, V.; Mennucci, B.; Cossi, M.; Scalmani, G.; Rega, N.; Petersson, G. A.; Nakatsuji, H.; Hada, M.; Ehara, M.; Toyota, K.; Fukuda, R.; Hasegawa, J.; Ishida, M.; Nakajima, T.; Honda, Y.; Kitao, O.; Nakai, H.; Klene, M.; Li, X.; Knox, J. E.; Hratchian, H. P.; Cross, J. B.; Bakken, V.; Adamo, C.; Jaramillo, J.; Gomperts, R.; Stratmann, R. E.; Yazyev, O.; Austin, A. J.; Cammi, R.; Pomelli, C.; Ochterski, J. W.; Ayala, P. Y.; Morokuma, K.; Voth, G. A.; Salvador, P.; Dannenberg, J. J.; Zakrzewski, V. G.; Dapprich, S.; Daniels, A. D.; Strain, M. C.; Farkas, O.; Malick, D. K.; Rabuck, A. D.; Raghavachari, K.; Foresman, J. B.; Ortiz, J. V.; Cui, Q.; Baboul, A. G.; Clifford, S.; Cioslowski, J.; Stefanov, B. B.; Liu, G.; Liashenko, A.; Piskorz, P.; Komaromi, I.; Martin, R. L.; Fox, D. J.; Keith, T.; Al-Laham, M. A.; Peng, C. Y.; Nanayakkara, A.; Challacombe, M.; Gill, P. M. W.; Johnson, B.; Chen, W.; Wong, M. W.; Gonzalez, C.; Pople; J. A. Gaussian 03, revision D.01; Gaussian, Inc.: Wallingford, CT, **2004**.
(11) Gavezzotti, A. Z. Kristallogr. 2005, 220, 499–510.
(12) Gavezzotti, A. *OPiX: A computer program package for the calculation of intermolecular interactions and crystal energies*, University of Milan: Italy, 2003.
(13) Gavezzotti, A. *J. Phys. Chem. B* **2002**, *106*, 4145–4154.
(14) Kunitski, M.; Riehn, C.; Matylitsky, V. V.; Tarakeshwar, P.; Brutschy, B. *Phys. Chem. Chem. Phys.* **2010**, *12*, 72–81.